Int. J. Heat Mass Transfer. Vol. 7, pp. 143–158. Pergamon Press 1964. Printed in Great Britain

LOCAL HEAT-TRANSFER COEFFICIENTS ON A UNIFORMLY HEATED CYLINDER

H. C. PERKINS Jr. and G. LEPPERT

Department of Mechanical Engineering, Stanford University, Stanford, California

(*Received* 25 *March* 1963 *and in revised form* 1 *July* 1963)

Abstract—Local heat-transfer coefficients from a uniformly heated cylinder with water in cross flow are presented and compared with analytical predictions. The influence of channel blockage is investigated and a correction presented for the effect of blockage on both the local and average heat transfer. The variation of viscosity with temperature across the boundary layer is also considered and its effect empirically correlated by means of a viscosity ratio.

Reynolds numbers from 2000 to 120 000; Prandtl numbers from 1 to 7; surface-to-bulk temperature differences from 20 to 120 degF; and blockage ratios from 0·208 to 0·415 were used in these tests. Local heat-transfer coefficients were determined by measuring the temperature variation of the tube wall with a thermocouple welded to the inner surface.

Analysis of the heat transfer in the laminar boundary layer uses integral methods with the Pohlhausen velocity profile in the momentum boundary layer and a third order temperature profile in the thermal boundary layer. A comparison is made between these results and previously published methods for the case of constant heat flux at the wall.

NOMENCLATURE

a, cylinder radius;
b, distance between dipoles;
C_D, drag coefficient;
C_p, pressure coefficient;
D, tube diameter;
D/W, blockage ratio;
h, heat-transfer coefficient;
$\bar{h}$, average heat-transfer coefficient with respect to angle;
k, thermal conductivity;
M, dipole moment;
m, ratio of thermal to hydrodynamic boundary layer thicknesses;
$\bar{N}_{Nu}$, average Nusselt number, $\bar{h}D/k$;
N_{Nu}, local Nusselt number, hD/k;
N_{Pr}, Prandtl number, $\mu C_p/k$;
N_{Re}, Reynolds number, $U_\infty D\rho/\mu$;
N_{Re}^*, blockage corrected Reynolds number, $U_\infty^* D\rho/\mu$;
p, pressure;
q'', heat flux;
T, free stream temperature at edge of boundary layer;
t, temperature;
U, free stream velocity at edge of boundary layer;
U_∞, free stream velocity upstream of test element;
U^*, blockage corrected velocity;
U', velocity ratio, U/U_∞;
u, velocity component in x direction;
v, velocity component in y direction;
v_θ, velocity component along cylinder wall;
W, duct width;
w, complex potential.

Greek symbols
α, thermal diffusivity;
Δ, thermal boundary layer thickness;
δ, velocity boundary layer thickness;
δ^*, displacement thickness;
θ, angle;
θ', momentum thickness;
λ, pressure gradient parameter;
μ dynamic viscosity;
ν, kinematic viscosity;
ρ, density;
τ, fluid shear stress;
ψ, stream function.

Subscripts
b, bulk;
w, wall;
∞, free stream value.

WHILE much work has been done on both the hydrodynamic and heat-transfer aspects of flow around cylinders, little has been done with liquids. In particular, for liquids, there have been few heat-transfer investigations using large temperature differences. Consequently, the effect of liquid property variations across the boundary layer has not been determined. Furthermore, little work has been done on the effect that channel blockage has on either the hydrodynamic or heat-transfer problems. It is known that when the cylinder takes up a large amount of the channel, that is, at high blockages, effects on pressure distribution, transition, separation point, and local heat transfer occur. This paper describes the effects of the temperature dependence of viscosity and of various blockage ratios on the local heat transfer from a cylinder. In addition, a correction to the average heat-transfer coefficient for the effect of blockage is discussed. With the exception of a few tests made at high velocity and high blockage, all runs were with a laminar boundary layer on the front portion of the tube and a subsequent laminar separation. The variation of the wall-to-bulk temperature difference produced a variation in the ratio of the viscosity at the wall to the bulk viscosity from 1·0 to 0·45.

The problem was treated analytically insofar as it was possible to do so. A prediction was made for the local heat transfer in the laminar boundary layer region of the tube based upon integral methods using polynomials for the velocity and temperature profiles across the boundary layer. In the region of separation no theoretical method exists for predicting the variation of heat transfer with angle. Consequently, an empirical correlation of the heat-transfer coefficient was all that could be accomplished in this region. It was possible, using potential flow theory, to examine the effect of blockage on the hydrodynamic behavior over the front half of the cylinders. Both potential flow and experimental pressure distributions were used to investigate and correlate the effect of blockage on the velocity and heat-transfer distributions. The problem of the viscosity variation across the boundary layer was treated in an empirical manner through the use of a viscosity ratio in the correlations.

Both the cases of heat transfer from a cylinder with a constant wall temperature and with a constant heat flux have been previously investigated. Some mass-transfer work has also been done with cylinders, and the analogy between mass and heat transfer has been used to study the heat transfer problem. In general, however, there has been little work done on cylinders with constant heat fluxes and no work done on the problem of local heat transfer for liquid coolants.

The problem of average heat-transfer coefficients from cylinders with liquid coolants has been treated by Perkins and Leppert [1], while several investigators have done work on local heat-transfer coefficients using air as the cooling fluid. Giedt [2] and Seban [3] have dealt with the case of a constant wall heat flux, while for the case of constant wall temperature, the standard work in the field is that of Schmidt and Wenner [4]. Zapp [5] has done extensive work on the influence of free stream turbulence on the local heat transfer from an isothermal cylinder, and Schlichting [6] includes some data by Kestin, Maeder and Sogin [7] for this same problem.

Several authors have discussed analytical predictions for the heat transfer through a laminar boundary layer. A short literature review with recommendations for the best methods has been made by Seban and Chan [8]. This includes the method of Lighthill [9] as well as those of Seban, all of which are applicable to the constant heat flux case. Several authors have presented methods which are useful for the constant temperature case or which may be extended to the condition of a variable wall temperature; see, for example, the recent paper by Spalding and Pun [10] which deals solely with the case of the isothermal wall. While all of the above mentioned methods may be used with any Prandtl number fluid, they were developed for the most part for air. As a consequence the Prandtl number dependence is not always clearly presented, but rather is given either in tabular form or is taken arbitrarily as the Prandtl number to the 0·4 or 0·33 power. Except reference [8], none of the above work includes any variable property effects.

EXPERIMENTAL APPARATUS

The heat-transfer loop in which the experimental data were obtained provides a test channel 7·97 in wide by 1·204 in deep [11]. Local heat transfer test elements consisted of thin wall, type 347 stainless steel tubes, about 2 in long, mounted directly in the channel and heated resistively by direct current. The wall thicknesses used were 0·005, 0·006, and 0·010 in. The power supply was a 750 A d.c. welding generator, modified to provide control over an extended current range. The current through the test section and the voltage drop across it were measured with calibrated instruments of ½ per cent accuracy.

The temperature of the inside wall was measured as a function of angle by spot-welding an iron-constantan thermocouple directly to the wall. The thermocouple was then covered with an insulating layer of ceramic cement to protect the thermocouple and to reduce natural convection effects.

Test sections for pressure distribution were made with a 0·010 in hole drilled directly through the tube which was then used as a local pressure measuring device. Static pressure was taken from a tap on the test channel and the difference read directly on a manometer. For combined heat transfer and pressure measurements a special tube was fabricated with a pressure tap which isolated the water column from the inside of the tube.

ANALYSIS

Potential theory

The pressure coefficient at the surface of a cylinder in an infinite stream is found from potential theory to be [12]

$$C_p \equiv \frac{P - P_\infty}{\rho U_\infty^2/2} = 1 - 4\sin^2\theta$$

while the potential flow solution for a cylinder in a duct is more complicated. Both Streeter [12] and Kotschin, *et al.* [13] treat this problem in limited ways. The latter point out that a system of infinitely many dipoles (i.e. doublets) superimposed on a uniform flow field leads to this case. They give the complex potential for the system of dipoles as

$$w = \frac{M}{2b}\coth\frac{\pi z}{b}$$

where M is the dipole moment and b is the distance between dipoles. If we add to this the complex potential for uniform flow we then have

$$w = U_\infty z + \frac{M}{2b}\coth\frac{\pi z}{b}.$$

The complex velocity follows as

$$\frac{\partial w}{\partial z} = U_\infty - \frac{\pi M}{2b^2}\frac{1}{\sinh^2(\pi z/b)}.$$

The stagnation points are given by the equation

$$\sinh^2\frac{\pi z}{b} = \frac{M\pi}{2b^2 U_\infty}.$$

If we denote the value of z at the stagnation point by the cylinder radius a, the dipole moment has the value

$$M = \frac{2b^2 U_\infty}{\pi}\sinh^2\frac{\pi a}{b}.$$

The stream function follows as

$$\psi = U_\infty y - \frac{(bU_\infty/\pi)\sinh^2(\pi a/b)\sin(2\pi y/b)}{\cosh(2\pi x/b) - \cos(2\pi y/b)}.$$

We may now see how the case of a cylinder in a channel results from this by looking at the expression with $\psi = 0$ and by making the streamlines at $\pm b/2$ into the channel walls. For $\psi = 0$

$$y\left(\cosh\frac{2\pi x}{b} - \cos\frac{2\pi y}{b}\right) = \frac{b}{\pi}\sinh^2\frac{\pi a}{b}\sin\frac{2\pi y}{b}$$

which may be expanded to yield

$$\cosh\frac{2\pi x}{b} - \cos\frac{2\pi y}{b} = 2\sinh^2\frac{\pi a}{b} + (\text{terms in } y).$$

Kotschin *et al.* point out that this is the equation for an oval. We can find the semidiameter in x by taking $y = 0$ and that in y by taking $x = 0$. For $a < b/4$ the oval is very close to a circle. For example, at $a = b/4$ the semidiameter in x is $0{\cdot}254b$, in y it is $0{\cdot}250b$.

Thus, for a blockage ratio of less than 0·500, the oval is effectively a circular cylinder in the channel. The velocity, as given by potential flow at the surface of the cylinder is

$$v_\theta = \left(\frac{\partial\psi}{\partial r}\right)_{r=a} = U_\infty \sin\theta - \left(\frac{bU_\infty}{\pi}\sinh^2\frac{\pi a}{b}\right)\left(\frac{\cos[(2\pi a/b)\sin\theta](2\pi/b)\sin\theta}{\cosh[(2\pi a/b)\cos\theta] - \cos[(2\pi a/b)\sin\theta]}\right.$$
$$\left. - \left\{\frac{\sin[(2\pi a/b)\sin\theta]\{\sinh[(2\pi a/b)\cos\theta](2\pi/b)\cos\theta + \sin[(2\pi a/b)\sin\theta](2\pi/b)\sin\theta\}}{\{\cosh[(2\pi a/b)\cos\theta] - \cos[(2\pi a/b)\sin\theta]\}^2}\right\}\right).$$

This expression may be used to find the velocity and pressure distribution as a function of angle and blockage ratio with the results shown in Fig. 1.

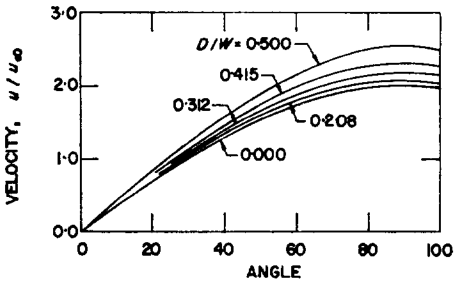

FIG. 1. Potential flow velocity distributions for flow around a cylinder in a restricted channel.

In the case of real flow, the inability of the laminar boundary layer to overcome the adverse pressure gradient causes it to separate near 90° and thus causes the pressure distribution to change from that of potential flow. On the front part of the cylinder where a stable laminar layer occurs the agreement between potential theory and experiment is substantial.

Heat transfer analysis

The laminar boundary layer analysis which will be presented is similar to that used by Brown *et al.* [14] to predict the heat transfer from a sphere. The momentum equation in integral form is set up with a fourth order velocity profile, the Pohlhausen profile, and is then solved by the Holstein–Bohlen technique [6] for the given external velocity distribution. The integral energy equation is then solved, in this case with a third order temperature profile, to yield the Prandtl number effect on the heat transfer. It is then possible to utilize the results of both the momentum and energy solutions to find the Nusselt number variation with angle.

Schlichting gives the integral momentum equation for the boundary layer in the form

$$U^2\frac{d\theta'}{dx} + (2\theta' + \delta^*)U\frac{dU}{dx} = \frac{\tau_w}{\rho} \qquad (1)$$

where δ^* and θ' are the displacement and momentum thicknesses, respectively. This form of the equation is derived based upon a rectangular geometry. The effect of the curvature of the cylinder is negligible, however, since the equation holds also for cases with no discontinuities in curvature [6].

With a fourth order velocity profile

$$u = a_0 + a_1 y + a_2 y^2 + a_3 y^3 + a_4 y^4 \qquad (2)$$

and the boundary conditions

$$y = 0: \quad u = 0, \quad \nu\frac{\partial^2 u}{\partial y^2} = \frac{1}{\rho}\frac{dp}{dx} = -U\frac{dU}{dx}$$

$$y = \delta: \quad u = U, \quad \frac{\partial u}{\partial y} = 0, \quad \frac{\partial^2 u}{\partial y^2} = 0$$

if it possible to solve equation (1) in a straightforward manner. The form parameter λ will be needed in the solution for the energy equation and is defined as

$$\lambda = \frac{\delta^2}{\nu}\frac{dU}{dx}.$$

The Holstein–Bohlen method of solution was programmed for a digital computer so the variation of the form parameter λ with angle could be readily determined for the many different external velocity distributions. Turning to the energy integral equation, we have

$$\frac{d}{dx}\int_0^\Delta (T - t)u\, dy = \alpha\left(\frac{\partial t}{\partial y}\right)_w = -\frac{q''}{\rho C_p}. \qquad (3)$$

A third order temperature profile is chosen with the boundary conditions:

$$t = b_0 + b_1 y + b_2 y^2 + b_3 y^3 \qquad (4)$$

$$y = 0: \quad \frac{dt}{dy} = -\frac{q''}{k}, \quad \frac{d^2 t}{dy^2} = 0$$

$$y = \Delta: \quad t = T, \quad \frac{dt}{dy} = 0.$$

The boundary condition on d^2t/dy^2 follows from the differential form of the energy equation with viscous dissipation neglected. A third order profile is chosen since this enables one condition on the second derivative of temperature to be used.

If the boundary conditions are applied to the profile there results

$$\frac{3(t-T)k}{2\Delta q''} = 1 - \frac{3}{2}(y/\Delta) + \frac{1}{2}(y/\Delta)^3. \qquad (5)$$

This may now be substituted directly into the integral in equation (3) along with the velocity profile. With this done, we have

$$I \equiv \int_0^\Delta u(y)\left\{\frac{2\Delta q''}{3k}\left[1 - \frac{3}{2}(y/\Delta) + \frac{1}{2}(y/\Delta)^3\right]\right\} dy. \qquad (6)$$

The integral energy equation is now in the form

$$\frac{dI}{dx} = \frac{q''(x)}{\rho C_p} \qquad (7)$$

which for the case of known heat flux may be integrated

$$I = \frac{1}{\rho C_p}\int_0^x q''(x)\, dx.$$

In making the integration of equation (6) the assumption has been made that $\Delta < \delta$. This restricts the analysis to cases of $N_{Pr} \geqslant 1$. However, for gases ($N_{Pr} = 0{\cdot}7$) the error will be small.

In complete form for the case of constant heat flux we have

$$\frac{2U\Delta^2 q''}{3k}\left[\frac{12+\lambda}{60}(\Delta/\delta) - \frac{\lambda}{48}(\Delta/\delta)^2 - \frac{3(4-\lambda)}{280}(\Delta/\delta)^3 + \frac{(6-\lambda)}{480}(\Delta/\delta)^4\right] = \frac{q''x}{\rho C_p}. \qquad (8)$$

Now, dividing both sides of this equation by $\delta^2 = \lambda\nu/dU/dx$ and letting the ratio of the boundary thicknesses, Δ/δ, be designated by m, we obtain

$$m^3\left[\frac{12+\lambda}{60} - \frac{\lambda}{48}m - \frac{3(4-\lambda)}{280}m^2 + \frac{6-\lambda}{480}m^3\right] = \frac{3x\,\alpha\, dU/dx}{2\lambda U\nu}. \qquad (9)$$

Since ν/α is the Prandtl number, this equation relates the ratio of the boundary layer thicknesses to the Prandtl number as a function of angle. This equation can now be solved for various Prandtl numbers using the values of λ determined previously at each angle.

At the stagnation point it is possible to pass over to the limit as x goes to 0 using L'Hopital's rule. Doing this and using the known value of λ at the stagnation point of 7·052, we obtain the right side of this equation as $0{\cdot}212/N_{Pr}$. We can then solve for m as a function of Prandtl number to obtain the results at the stagnation point as: N_{Pr} equals 1·0, 10·0, 100·0; m equals, respectively, 1·018, 0·434, 0·194.

A function of the form $m = aN_{Pr}^{-b}$ can be fitted to these points to give a relationship between the Prandtl number and the ratio of the boundary layer thicknesses at the stagnation point. This dependence may be determined at other values of angle in a similar manner. A value for b of 0·36 was used throughout the present analysis for all positions of angle and all heat-transfer distributions, although the analytically determined values reached as low as 0·34 in some cases at an angle of 80°.

With m determined as a function of angle and the fluid boundary layer thickness known from the solution of the momentum equation, it is possible to predict the local heat transfer

$$q''/h = t_w - T = \frac{2q''\Delta}{3k} = \frac{2q''m\delta}{3k}$$

or

$$N_{Nu} = hD/k = 3D/2m\delta. \qquad (10)$$

Equation (10) may be put into a more convenient and useful form by using some of the previous definitions. Since $\delta^2 = \lambda\nu/dU/dx$ and $m = aN_{Pr}^{-b}$ we have

$$N_{Nu} = \frac{3DN_{Pr}^b}{2a}\sqrt{\left(\frac{dU/dx}{\lambda\nu}\right)}. \qquad (11)$$

Now the Reynolds number is $N_{Re} \equiv U_\infty D/\nu$ and

$$dU/dx = \frac{dU}{d\theta}\frac{d\theta}{dx} = \frac{2}{D}\frac{dU}{d\theta}$$

so that

$$N_{Nu} = \frac{3}{2a} N_{Pr}^{b} N_{Re}^{0.50} \sqrt{\left(\frac{2\,dU'/d\theta}{\lambda}\right)} \quad (12)$$

where U' is the ratio U/U_{∞}.

For the case of potential flow, with no blockage, we know that $U = 2U_{\infty} \sin\theta$ and $dU'/d\theta = 2\cos\theta$, so that equation (12) reduces to

$$N_{Nu} = \frac{3}{a}\left(\frac{\cos\theta}{\lambda}\right)^{1/2} N_{Pr}^{b} N_{Re}^{0.50}. \quad (13)$$

At the stagnation point of an isothermal circular cylinder, Squire [15] has predicted that the Nusselt number has the value

$$N_{Nu} = 1.14\, N_{Pr}^{0.40} N_{Re}^{0.50}, \quad 0.6 < N_{Pr} < 2.0.$$

If the velocity distribution which results from extrapolating the experimental velocity distributions to a zero blockage ratio is used, as is described in the Discussion, equation (12) gives at the stagnation point of a cylinder with constant heat flux

$$N_{Nu} = 1.08\, N_{Pr}^{0.36} N_{Re}^{0.50}.$$

Thus the stagnation point results of the integral analysis for constant heat flux compare favorably with those of the isothermal case.

Using equation (12) with the necessary velocity distributions and the values of λ determined from the Holstein–Bohlen momentum equation solution, one can predict the local heat transfer over the laminar region of the cylinder. Fig. 6a shows the results of this prediction which do not, of course, include effects of free stream turbulence.

EXPERIMENTAL RESULTS

Because the tube was heated resistively with direct current, the thermocouple welded directly to the inner surface was subject to electrical pickup. A technique to measure this pickup has been described by Davenport *et al.* [16] and was used in correcting the observed thermocouple emf.

Local temperature measurements were made by rotating the tube in 10° increments and observing the continuous trace on an oscillograph. It was necessary to use a recording instrument for the temperature since on the rear part of the tube, in the separated region, the temperature underwent rapid and large fluctuations. These could not be read on a manually balanced potentiometer, nor could an adequate average temperature be determined from these fluctuations by using a static temperature measuring device. The oscillograph therefore provided not only the temperature–time dependence at each angle in the separated region but also provided an accurate way to determine the time-averaged temperature on that part of the tube. The local heat-transfer coefficient was then determined from the wall temperature and the heat flux.

Fluid properties for water were taken from the tabulation in [17]. The correction for the temperature drop through the wall was made on the basis of constant metal properties, since the temperature drop through the wall was small, at most 13 degF. There was negligible conduction in the axial direction of the tube because of the small cross-sectional area involved and because the electrodes were at the bulk fluid temperature, so that the axial temperature difference was not large.

Giedt [18] has discussed a method of correcting for conduction in the angular direction. Since for our results this correction is very small, 1 to 2 per cent, and applies to only one or two points on each run, it was not made in the final tabulation of the data.

The velocity was determined from the orifice measurements of the flow rate. In addition to correcting this for the effect of tube blockage, it is also desirable to correct for the velocity profile if this is not flat. For the present experiment the unobstructed channel center line velocity was assumed to be the appropriate velocity to be used in the Reynolds number. Reference [1] discusses in greater detail the correction for the effect of the channel velocity profile.

Some of the results of the pressure measurements are shown in Fig. 2 in terms of the local velocity around the tube. The effect that blockage has on the velocity distribution is evident from this figure.

In all runs, the measured wall temperature rises smoothly from the stagnation point to near the 80° position as the laminar boundary layer

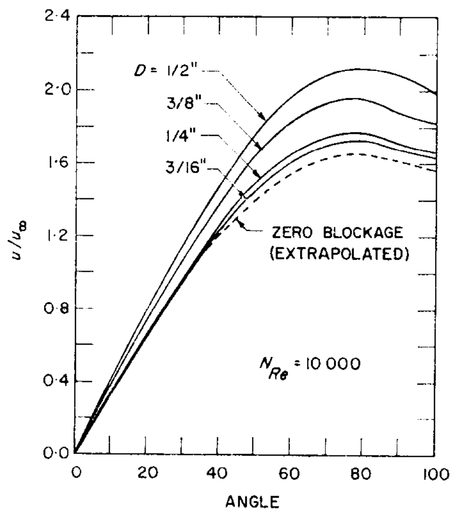

FIG. 2. Experimental velocity distributions for flow around various sized cylinders in a restricted channel.

gradually thickens. Fig. 3 shows the effect of this temperature rise on the variation of the parameter $N_{Nu}/N_{Re}^{0.50}N_{Pr}^{0.36}$ for the three tube sizes tested. For all three of these sets of data, the average temperature differences are small, approximately 30 degF, and the Reynolds number is constant. The spread of these curves, therefore, reflects the effect of differing degrees of channel blockage.

The primary reason that convective heat transfer is different for liquids than for gases is that the viscosity of most liquids decreases markedly with temperature. Consequently, the constant properties analysis of the heat-transfer

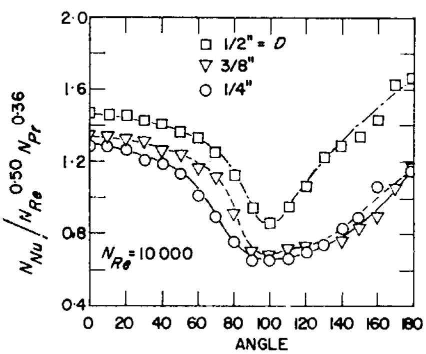

FIG. 3. Local heat-transfer coefficients on various sized circular cylinders.

behavior is inadequate except for very small temperature differences.

An empirical correction factor consisting of a viscosity ratio with an appropriate exponent was first suggested by Sieder and Tate [19] and has been applied successfully to correlate average heat-transfer coefficients from cylinders to liquids [1]. The same correlating factor has been applied to the present local heat-transfer results, with typical effectiveness as shown by Fig. 4. The wall viscosity here was evaluated at the local wall temperature, and $\overline{\Delta T}$ refers to the angle-averaged temperature difference across the boundary layer.

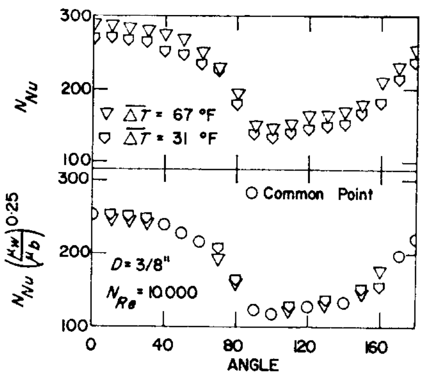

FIG. 4. Data corrected for the variation of viscosity with temperature using the ratio $(\mu_w/\mu_b)^{0.25}$.

Schlichting [6] shows from the boundary layer equations that the heating or cooling of a body should have some effect on the stability of the boundary layer. For heating a liquid, the boundary layer should be stabilized because the viscosity decreases with temperature. Therefore, it would seem that pressure distributions taken with heating should be used in any prediction for the laminar boundary layer heat transfer. In order to investigate this a pressure tap was fitted to a half-inch tube and measurements were taken of the pressure distribution with and without heating. No significant differences were found over the laminar boundary layer region. It thus appears that any changes in the pressure distribution with heating, in the forced convection region, are not important to the prediction of the heat transfer over the laminar portion of the tube. However, as Schlichting suggests, and as the data seemed to support, heating may affect both the pressure distribution near the separation point and also the location of the transition point when the Reynolds number is near the critical value.

DISCUSSION AND COMPARISON

Channel blockage

Fig. 3 shows that the blockage has a significant influence on the heat transfer because of its effect on the velocity distribution around the cylinder. As expected, a high blockage markedly increases the velocity around the cylinder. The separation point is also blockage-dependent, as is the critical Reynolds number. It appears from the experimental pressure and velocity distributions that a high blockage causes separation to take place at a later point than would occur with no blockage. Also with increasing blockage the velocity distributions are more like those predicted from potential flow.

There are at least two approaches that can be taken to correct for blockage. Robinson *et al.* [20] have chosen to correct the Nusselt number with a correlating factor from different blockage ratios, whereas Vliet and Leppert [21] have attempted to find a new Reynolds number to correlate the blockage effect. In the latter approach some factor is sought which will change the Reynolds number so that the heat-transfer results at different blockages are all correlated onto one curve. Since it is the velocity which is first affected by the blockage, it seems more appropriate to correct the Reynolds number.

It is possible to cross plot, for various angular positions, the experimental velocity distributions from Fig. 2 as a function of blockage to extrapolate to a "zero-blockage" velocity distribution. This distribution, which would be expected to exist around the cylinder for a zero blockage ratio, i.e. in an infinite channel, is used to determine the correction for the effect of blockage on the heat transfer. To eliminate the effect of blockage one can correct the free stream velocity, used in the Reynolds number, by multiplying by the ratio of the local velocity on the cylinder with blockage to that which would exist without blockage. Thus the Reynolds number to be used in correlating the local data is given as

$$N_{Re}^{*} = \frac{D U_{\infty}}{\nu} \frac{U(\theta)_{\text{finite blockage}}}{U(\theta)_{\text{zero blockage}}} = N_{Re} \frac{U(\theta)_{\text{finite blockage}}}{U(\theta)_{\text{zero blockage}}}$$

Calculated values of this velocity ratio are shown in Fig. 5.

In spite of the fact that the local pressure measurements do not have a corresponding velocity at angles beyond the separation angle, corrections are shown on this figure for angles greater than θ_{sep}. These were calculated as if a velocity exists in the separation region of the cylinder. However, the corrections also are the same as

$$\sqrt{[1 - C_p(\theta)]}/\sqrt{[1 - C_p(\theta)]_{\text{zero blockage}}}.$$

We can now attempt to eliminate the influence of blockage on the predicted Nusselt numbers of

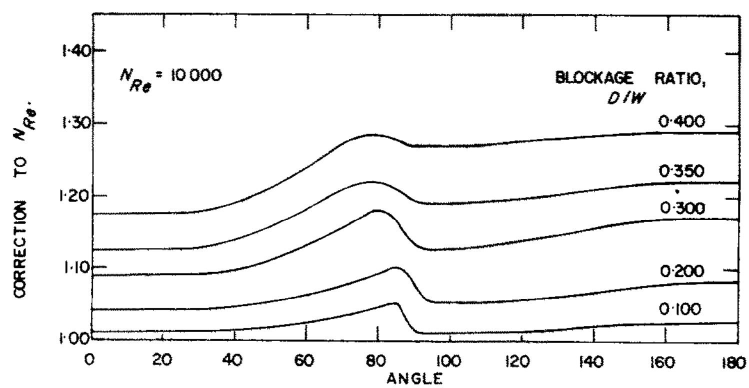

FIG. 5. Local corrections for Reynolds number for cylinder blockage in a channel, based on experimental pressure distributions.

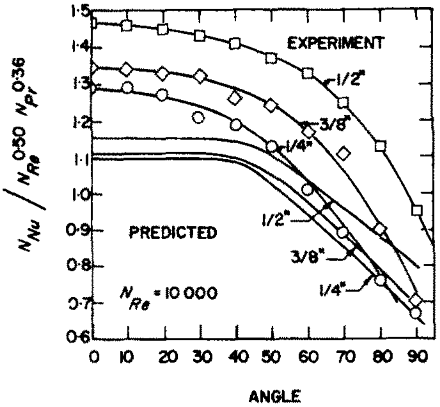

FIG. 6a. Prediction of Nusselt number, not blockage corrected, and experimental results for a cylinder in cross flow.

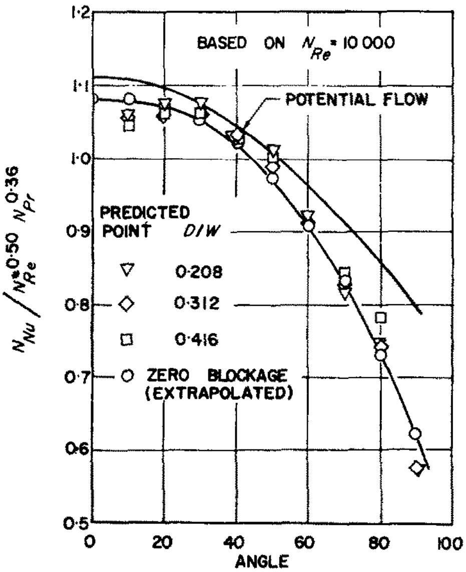

FIG. 6b. Prediction of Nusselt number, blockage corrected, for a cylinder in cross flow.

Fig. 6a by using the corrected Reynolds number. If the correction is effective, the result should be a single distribution of Nusselt number applicable to all three tube sizes. Fig. 6b shows such a distribution obtained from the three predicted Nusselt number distributions using a blockage-corrected Reynolds number, and it is seen that the different predictions do fall close to a single curve.

It should also be possible to predict the local heat transfer directly from the velocity distribution which was found from the extrapolation to zero blockage. A prediction has been made by the method described earlier in the analysis section using this velocity distribution, and the result appears in Fig. 6b. This Nusselt number distribution agrees with the blockage-corrected distributions, as it should, and illustrates the effectiveness of the method of correcting the Reynolds number for blockage. The same procedure can be followed using the potential flow results, in which case the zero blockage distribution is known analytically. Fig. 6b also includes the predicted heat-transfer coefficients based upon the potential flow velocity distribution around a cylinder in an infinite stream.

Using the area available for flow per unit length of cylinder, one can determine a local blockage correction geometrically, at least over the front half of the cylinder where the flow is not affected by the separation of the boundary layer and the formation of the wake.

The local area available to the flow per unit length of tube is $(W - D \sin \theta)$. Using the ratio of velocities with and without blockage as the correction term, we have:

$$\frac{U(\theta)}{U(\theta)_{\text{block}=0}} = \frac{W/D}{W/D - \sin \theta}.$$

It is found that the corrections determined in this manner are higher than those found from experiment except near the stagnation point. Thus the simple geometrical correction appears to undercorrect near the stagnation point and to overcorrect further around the cylinder, as is indeed the case when this correction is applied to the experimental data and to the predicted Nusselt number distributions. Consequently, the use of the geometrical blockage correction is not recommended.

Next consider the correction which should be used with the average heat-transfer coefficients. One manner of correction is to use the linear average, taken over the cylinder circumference, of the local corrections. Since it is not possible to justify this analytically we can justify it only in an empirical way.

The averages of the local corrections for a Reynolds number of 10^4 are shown in Table 1 for various sectors of a cylinder. If these are

Table 1. Average blockage corrections

	Determined from average value of the local corrections					Determined from the integrated value of the predicted Nusselt numbers		
	Blockage ratio					Blockage ratio		
Cylinder Sector	0·0	0·100	0·200	0·300	0·400	0·208	0·312	0·415
0–80°	1·000	1·014	1·046	1·112	1·215	1·065	1·119	1·220
90–180°	1·000	1·018	1·071	1·149	1·268			
0–180°	1·000	1·016	1·058	1·133	1·244			

the proper corrections to be used, they should correlate the average of the locally predicted Nusselt numbers. To find the average of these, the local heat-transfer distributions were integrated graphically over the first 80° to obtain the average value for the heat-transfer coefficient over this sector. The corrections to the Reynolds number required to correlate these average Nusselt numbers onto the values found from the zero-blockage distribution are also given in Table 1. The corrections determined from the heat-transfer distributions fall close to the curve found from the average local corrections, at least over the 0–80° sector of the cylinder. Lacking further information, one may suppose that since the method works in this region, it is then possible to approximate the average value correction for the whole cylinder in the same way.

Several factors for blockage correction for average heat-transfer coefficients from a cylinder are shown in Fig. 7. The mean area concept [21] leads to

$$A_{\text{mean}} = \frac{\text{channel volume} - \text{tube volume}}{\text{tube diameter}}.$$

It is thus defined as the ratio of the flow volume in the channel at the location of the body to the body height. For a cylinder,

$$A/A_{\text{mean}} = 4W/(4W - D).$$

Pope [22] suggests correcting for "solid blocking" and "wake blocking". He gives the correction to the velocity in the form

$$U^* = U_\infty \left[1 + 0{\cdot}822\left(\frac{D}{W}\right)^2 + \frac{C_D}{4}\left(\frac{D}{W}\right)\right]$$

where the second term corrects for solid blocking and the third term is for wake blocking. This form of correction is based upon the results of potential flow theory using the method of images. To obtain the curve in Fig. 7 a drag coefficient of 1·18 was used in this expression, which corresponds to a cylinder Reynolds number between about 10^2 and 2×10^5.

A third method of correction, described by Robinson *et al.* [20], was empirically determined from local heat-transfer data from cylinders with nonisothermal surfaces. The correction at the stagnation point was determined by correlating their results to those

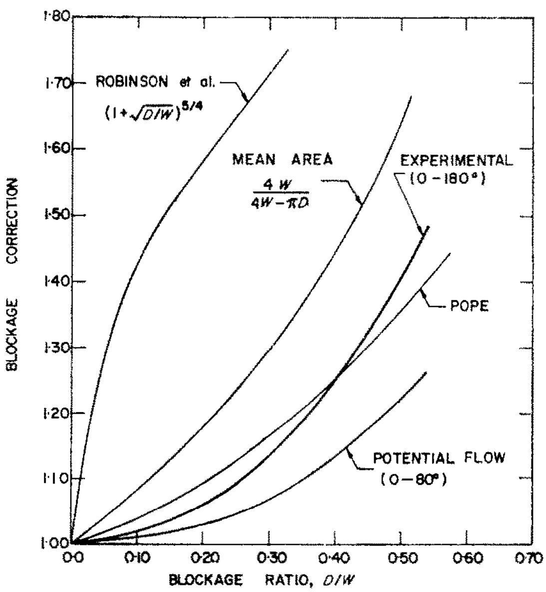

Fig. 7. Average blockage corrections for Reynolds number for cylinder blockage in a channel.

predicted by Squire [15] for the heat transfer at the stagnation point of an isothermal cylinder. To correlate these they multiply the Reynolds number by the empirically determined factor $[1 + \sqrt{(D/W)}]$. For the average heat-transfer coefficients over the cylinder they use the expression

$$N_{Nu} / [1 + \sqrt{(D/W)}] = C N_{Re}^{n}.$$

This is, of course, a correction factor applied to the Nusselt number, but it is equivalent to multiplying the Reynolds number by the factor $[1 + \sqrt{(D/W)}]^{1/n}$. For their data n varies from 0·53 to 0·806, while a value of 0·80 has been used in Fig. 7.

The average of the local correction found empirically falls below the previously used [1] mean area curve and far below the Robinson correction for all non-zero blockage ratios of interest. It agrees rather well with the correction suggested by Pope, and is greater than the prediction from potential flow.

The average correction is based upon velocity distributions for $N_{Re} = 10\,000$. However, the results are essentially the same for the $N_{Re} = 50\,000$ velocity distributions so that the correction should apply for $10\,000 < N_{Re} < 50\,000$. Furthermore, it should be applicable over the entire range of Reynolds numbers where a laminar separation occurs from the cylinder.

Local heat transfer

Fig. 8 shows the data of Fig. 6a corrected for blockage and compared with the zero blockage prediction. The data are about 20 per cent higher than the prediction. However, the scatter in the data is now about 7·5 per cent, whereas in Fig. 6a it was about 15 per cent. Therefore the recommended blockage correction markedly reduces the spread in the data.

For comparison to the authors' solution the methods of Seban [8], Lighthill [9] and Eckert [23] have been used to determine the local heat transfer from a cylinder. The latter method holds only for an isothermal cylinder, while the former two were applied for the case of a constant wall heat flux. The "effective shear stress" of Tifford [24] was used in the method of Lighthill. Both the analyses of Seban and Eckert are based on wedge flow profiles. The three

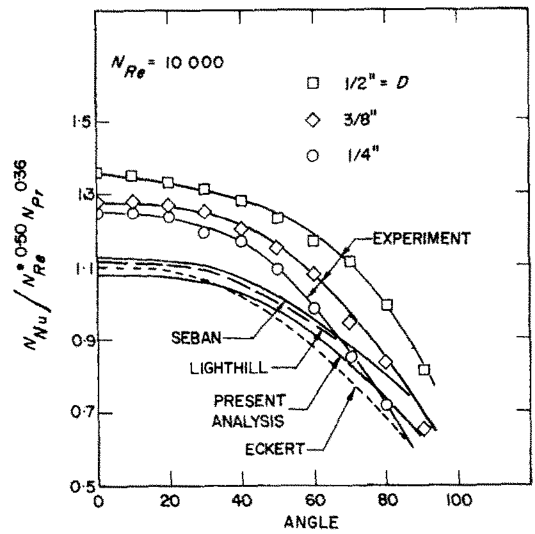

FIG. 8. Comparison of experimental values of local heat-transfer coefficients from a cylinder to predictions of various authors.

predictions for the constant heat flux boundary condition (Seban, Lighthill, present analysis) all have the same shape and lie within 4 per cent of one another, as shown in Fig. 8. The prediction by the method of Eckert, made on the basis of the isothermal wall condition, falls off more sharply with angle than the others.

A correlation of all the local heat transfer results is given in Fig. 9. This includes data for Reynolds numbers from 2700 to 103 000 and data from the $\frac{1}{4}$, $\frac{3}{8}$, and $\frac{1}{2}$ in tubes. Blockage corrections and variable viscosity corrections have been made so that the influence of these variables on the data should be minimized. The total scatter in the results is about $\pm 7·5$ per cent. It should be noted, however, that the data taken in several investigations [3, 4, 25] have shown a tendency to have an increasing value of $N_{Nu}/N_{Re}^{0·50}$ with an increasing Reynolds number. Reference [25] includes a brief discussion of this phenomenon. Consequently, some of the scatter in the data shown in Fig. 9 may be attributed to this increase in the ordinate as the Reynolds number is increased. For example, at the stagnation point the minimum experimental value of the ordinate, 1·12, is for a Reynolds number of 10 000, while the maximum value 1·29 is for a Reynolds number of 103 000. The ordinate

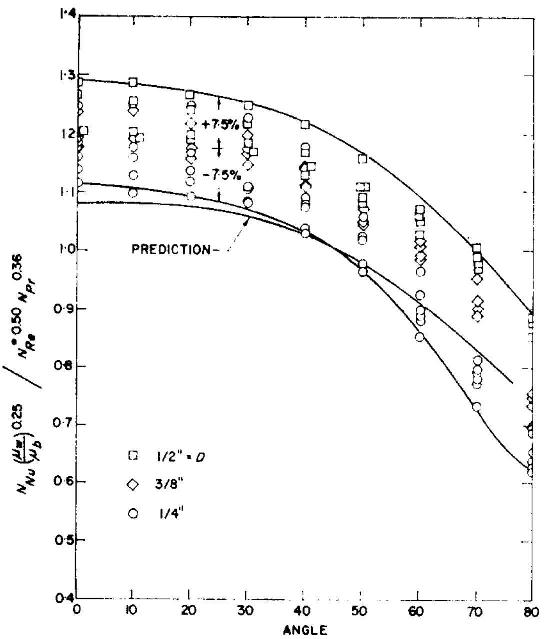

FIG. 9. Correlation for the laminar heat transfer from a cylinder, corrected for the influence of blockage and variable viscosity.

at the stagnation point for the minimum Reynolds number, 2700, is 1·14, which is next to the minimum value. Included in the figure for reference is the prediction made with the extrapolated zero blockage velocity distribution.

Turbulence

It is well known [3, 5, 6, 7, 26] that the turbulence level has a large influence on the heat transfer from bodies in external flow. This is true for both the average heat transfer [6, 26] and the local heat transfer [3, 5, 6, 7]. Consequently, measurements were taken with a constant temperature, hot film anemometer to find the turbulence level in the test channel in the direction of the bulk flow. The data indicate an average turbulence level of 2·9 $\pm$ 0·5 per cent, which would seem to indicate that there is a high turbulence level in the test channel and that, therefore, the heat transfer should be grossly affected. However, the heat transfer results, both average [1] and local, appear to be more in line with a 1 per cent turbulence level, as we shall demonstrate.

The lack of agreement between the predictions and the experimental results in Figs. 8 and 9 is probably due to the influence of free stream turbulence. In order to investigate some aspects of the relationship between heat transfer and turbulence, it is of interest to compare data from the several investigators who have worked on this problem. Fig. 10 shows experimental results

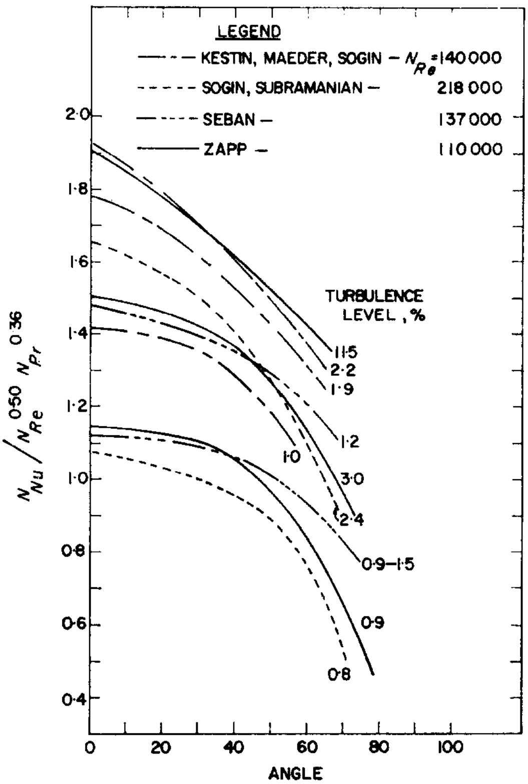

FIG. 10. Turbulence effects on the heat and mass transfer from a circular cylinder.

for the local heat or mass transfer as affected by the turbulence level. The inconsistency of the results is obvious. Fig. 11 shows these results normalized on the predicted Nusselt number. Included on the same figure are representative data from the present investigation. We see that the turbulence intensity seems to have little effect on the results of Seban [3] and of Sogin and Subramanian [25] until it becomes greater than about 1 per cent; however, the data of Kestin *et al.* [7] exhibit a large effect even at a 1 per cent turbulence intensity. Zapp's data [5] are not included since he made no prediction for the heat-transfer distribution. It is of interest to note that Kestin's data [7] and Sogin's data [25] were obtained in the same wind tunnel.

It is possible that there are more effects here than just the changing turbulence intensity. For example, the scale or spectral distribution of turbulence may also have some effect, although the scale should have little effect provided that it is small in comparison with the size of the body. Such should be the case in all of the above experiments. The spectral distribution as a function of wave length has been measured only by Seban [3], who found that some effect appears to exist but was unable to go into any further detail.

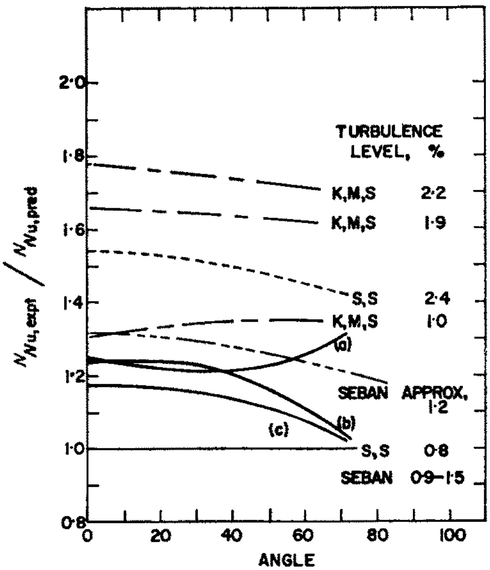

FIG. 11. Comparison of the ratio of experimental to predicted Nusselt numbers—*a*, *b*, *c* from present experiment. For legend see Fig. 10.

One of the reasons for the discrepancy in the different measurements may be the influence of the pressure distribution on the cylinder. This is, in turn, a function of the blockage. The blockage in the experiments discussed here was 0·139 for the Seban experiment, about 0·130 for Kestin *et al.* and for Sogin and Subramanian, 0·110 for Zapp's work and from 0·208 to 0·415 for the present work. Since the blockage is nearly the same in the first four experiments listed above, it would seem to be secondary in causing the different results.

In the absence of more detailed data and information it does not seem reasonable to attempt a correlation of the various experiments. The normalization in Fig. 11 should, however, reduce the differences which may be caused by dissimilar thermal boundary conditions and should present the data conveniently for a comparison of the turbulence effects.

In general, it appears that turbulence causes the greatest increase in heat transfer near the stagnation point [3, 7, 25]. The data of the present experiment also seem to indicate this. It would seem that the discrepancy between the predictions and results of the present experiment is caused by the free stream turbulence. Unfortunately, it is not yet possible to obtain even an empirical correlation for this effect because of the large differences between the various experiments. From the presentation of the data in Fig. 11, one would expect that the turbulence level in the present experiment is of the order of 1 per cent, which is much lower than the measured value of 2·9 per cent.

The turbulence level may also be predicted in a semi-empirical fashion based upon the work of Batchelor and Townsend [27]. In this manner the intensity is estimated as about 1·1 per cent [1]. The cause of the disagreement between the measured level of 2·9 per cent and the "predicted" level of 1·1 per cent is not known. However, the disparity may be due to the effect of the channel walls in the relatively narrow channel.

Average heat transfer

Perkins and Leppert [1] include extensive results for the average heat-transfer coefficient from a cylinder which were corrected for blockage using the mean area correction. The additional data available in the present work have led to a more accurate experimental correction for blockage (Fig. 7) based upon the measured pressure distributions.

The difference between the new blockage correction and the mean area correction is small; however, new correlations were determined in the same form as the previous ones. These are

$$\overline{N_{Nu}}\left(\frac{\mu_w}{\mu_b}\right)^{0.25} \Big/ N_{Pr}^{0.40} = 0.31\, N_{Re}^{*0.50} + 0.11\, N_{Re}^{*0.67} \qquad (14)$$

and

$$\overline{N_{Nu}}\left(\frac{\mu_w}{\mu_b}\right)^{0.25} \Big/ N_{Pr}^{0.40} = 0.57\, N_{Re}^{*0.50} + 0.0022 N_{Re}^{*} \quad (15)$$

The earlier correlations used coefficients of 0·30 and 0·10 in place of the present 0·31 and 0·11 in equation (14) and 0·53 and 0·0019 in place of 0·57 and 0·0022 in equation (15). The integrated average values of the local heat-transfer coefficients obtained in this experiment agree closely with the previous data, which were based on a single temperature reading taken on the tube centerline. From the temperature traces around the cylinder it appears that each of the two modes of heat transfer observed here, i.e. laminar and separated, may be expected to occur over about half of the cylinder (assuming that the Reynolds number is below the critical value).

CONCLUSIONS

1. An additive type of correlation may be used to correlate average heat-transfer coefficients from a cylinder. The correlation which appears to be most satisfactory includes a term using $N_{Re}^{0.50}$ to account for the heat transfer in the laminar boundary layer region on the tube and a term using $N_{Re}^{0.67}$ to account for the heat transfer in the separated region. This correlation is given by equation (14).

2. The effect of the variation of viscosity across the boundary layer may be accounted for by using a ratio of the viscosity at the wall to the bulk viscosity in the experimental correlations for both the local and average heat-transfer coefficients.

3. The free stream turbulence intensity has a substantial influence on the heat transfer from a cylinder when the turbulence level is greater than 1 per cent.

4. A correction for the influence of blockage on both the local and average heat-transfer may be made by determining a blockage-corrected Reynolds number for use in the correlations.

5. There appears to be little difference between the predictions made by the present integral technique and by the methods of Seban and Chan [8] and Lighthill [9]. The integral method has the advantage of using polynomials for the velocity and temperature profiles across the boundary layers so that one can readily obtain an intuitive grasp of the boundary layer effects. However, the method of Seban is less lengthy to apply.

ACKNOWLEDGEMENTS

This paper is based on a dissertation [28] submitted to Stanford University by H. C. Perkins, Jr., in partial fulfillment of requirements for the degree of Doctor of Philosophy. Dr. Perkins was the holder of an Atomic Energy Commission Fellowship during part of this investigation. The work was supported by a research grant from the U.S. Army Research Office (Durham).

REFERENCES

1. H. C. PERKINS and G. LEPPERT, Forced convection heat transfer from a uniformly heated cylinder, *J. Heat Transfer, Trans. ASME*, **84**, 257–263 (1962).
2. W. H. GIEDT, Effect of turbulence level of incident air stream on local heat transfer and skin friction on a cylinder, *J. Aero. Sci.* **18**, 725–730, 766 (1951).
3. R. A. SEBAN, The influence of free stream turbulence on the local heat transfer from cylinders, *J. Heat Transfer, Trans. ASME*, **82**, 101–107 (1960).
4. E. SCHMIDT and K. WENNER, Heat transfer over the circumference of a heated cylinder in transverse flow. *NACA* TN 1050 (1943) (Translation from the original German article).
5. G. M. ZAPP, The effect of turbulence on local heat transfer coefficients around a cylinder normal to an air stream, M.S. Thesis, Oregon State College (1950).
6. H. SCHLICHTING, *Boundary Layer Theory*. Fourth Edition. McGraw-Hill, New York (1960).
7. J. KESTIN, P. F. MAEDER and H. H. SOGIN, The influence of turbulence on the transfer of heat to cylinders near the stagnation point, *J. Appl. Math. Phys.* (*ZAMP*) **12**, 115–132 (1961).
8. R. A. SEBAN and H. W. CHAN, Heat transfer to boundary layers with pressure gradients, WADC T.R. 57–111 (1958) (ASTIA AD 118–075).
9. M. LIGHTHILL, Contribution to the theory of heat transfer through a laminar boundary layer, *Proc. Roy. Soc.* **A202**, 359–377 (1950).
10. D. B. SPALDING and W. M. PUN, A review of methods for predicting heat-transfer coefficients for laminar uniform-property bouhdary layer flows, *Int. J. Heat Mass Transfer*, **5**, 239–249 (1962).
11. G. C. VLIET, Local boiling peak heat flux for water flowing normal to cylinders. Ph.D. Dissertation, Mechanical Engineering Department, Stanford University (1962).
12. V. L. STREETER, *Fluid Dynamics*. McGraw-Hill, New York (1948).
13. N. J. KOTSCHIN, I. A. KIBEL and N. W. ROSE, *Theoretische Hydromechanik*, Vol. 1. Akademie Verlag, Berlin (1954) (translated from Russian to German).
14. W. BROWN, C. C. PITTS and G. LEPPERT, Forced

convection heat transfer from a uniformly heated sphere to water, *J. Heat Transfer, Trans. ASME*, **84**, 133–140 (1962).
15. H. B. SQUIRE, *Modern Developments in Fluid Dynamics*, Vol. 2. Oxford University Press, London (1938).
16. M. DAVENPORT, P. MAGEE and G. LEPPERT, Thermocouple attachment to a direct-current heater, *J. Heat Transfer, Trans. ASME*, **84**, 187–188 (1962).
17. E. R. G. ECKERT and R. M. DRAKE, *Heat and Mass Transfer*. Second Edition. McGraw-Hill, New York (1959).
18. W. H. GIEDT, Investigation of variation of point unit heat transfer coefficient around a cylinder normal to an air stream, *Trans. ASME*, **71**, 375–381 (1949).
19. E. N. SIEDER and G. E. TATE, Heat transfer and pressure drop of liquids in tubes, *Industr. Engng. Chem.* **78**, 1429–1435 (1936).
20. W. ROBINSON, L. S. HAN, R. H. ESSIG and C. F. HEDDLESON, Heat transfer and pressure drop data for circular cylinders in ducts and various arrangements. Ohio State University Research Foundation, Report 41, 1951 (ASTIA ATI 128–961).
21. G. C. VLIET and G. LEPPERT, Forced convection heat transfer from an isothermal sphere to water, *J. Heat Transfer, Trans. ASME*, **83**, 163–175 (1961).
22. A. POPE, *Wind Tunnel Testing*. Second Edition. Wiley, New York (1954).
23. E. R. G. ECKERT, Die Berechnung des Wärmeüberganges in der Laminaren Grenzschicht Unströmter Körper, *VDI Forschungsheft* **416**, 13 (1942). (Calculation of the heat transfer in the laminar boundary layer of submerged bodies, translated by R. H. Kay, copies available from R. M. Drake, Princeton University, Princeton, New Jersey.)
24. A. TIFFORD, On the theory of heat transfer through a laminar boundary layer, *J. Aero. Sci.* **18**, 283–284 (1951). (See also WADC TR 53–288, part 5, The modified Lighthill method for determining the rate of heat transfer, 1954.)
25. H. H. SOGIN and V. S. SUBRAMANIAN, Local mass transfer from circular cylinders in cross flow, *J. Heat Transfer, Trans. ASME* **83**, 483–493 (1961).
26. J. KESTIN and P. F. MAEDER, Influence of turbulence on transfer of heat from cylinders. *NACA* TN 4018 (1957).
27. G. K. BATCHELOR and A. A. TOWNSEND, Decay of isotropic turbulence in the initial period, *Proc. Roy. Soc.* A, **193**, 539–558 (1948).
28. H. C. PERKINS, Forced convection heat transfer from a uniformly heated cylinder. Ph.D. thesis in Mechanical Engineering, Stanford University (1963).

Résumé—Les coefficients locaux de transfert de chaleur obtenus dan le cas d'un cylindre uniformément chauffé placé normalement à un écoulement d'eau sont comparés aux prévisions théoriques. L'influence du blocage de la conduite est étudié et on présente une correction, tenant compte de cet effet de blocage, valable à la fois pour les transmissions de chaleur locale et moyenne. La variation de la viscosité avec la température à travers la couche limite est également considérée et son effet traduit empiriquement au moyen d'un rapport de viscosité.

Dans ces essais, on a pris des nombres de Reynolds compris entre 2000 et 120000, des nombres de Prandtl de 1 à 7; des différences de température en surface et écoulement moyen de 11 à 67°C et des rapports de blocage de 0,208 à 0,415. Les coefficients locaux de transmission de chaleur ont été déterminés par la mesure de la variation de température de la paroi du cylindre à l'aide d'un thermocouple soudé sur sa face interne.

L'étude de la transmission de chaleur dans la couche limite laminaire utilise des méthodes intégrales avec le profil de vitesses de Pohlhausen dan la couche limite dynamique et un profil de température du 3° ordre dans la couche limite thermique. On fait une comparaison de ces résultats et de ceux des méthodes publiées précédemment dans le cas d'un flux de chaleur constant à la paroi.

Zusammenfassung—Örtliche Wärmeübergangskoeffizienten an einem gleichmässig beheizten, von Wasser querangeströmten Zylinder werden angegeben und mit analytischen Ergebnissen verglichen. Die Wirkung der Kanalverengung wurde untersucht und ihr Einfluss auf den örtlichen und mittleren Wärmeübergang in einer Korrektur ausgedrückt. Die Änderung der Zähigkeit in der Grenzschicht mit der Temperatur ist ebenfalls berücksichtigt und ihr Einfluss empirisch mit einem Zähigkeitsverhältnis eingeführt.

Reynoldszahlen von 2000 bis 120 000; Prandtlzahlen von 1 bis 7; Differenzen zwischen Oberflächen- und Mitteltemperatur von 11 bis 67 grd, und Verengungsverhältnisse von 0,208 bis 0,415 lagen den Versuchen zugrunde. Örtliche Wärmeübergangskoeffizienten wurden durch Messung der Änderung der Rohrwandtemperatur mit einem an die Innenwand gelöteten Thermoelement bestimmt.

Eine Analyse des Wärmeübergangs in der laminaren Grenzschicht beruht auf Integralmethoden mit dem Geschwindigkeitsprofil von Pohlhausen in der Impulsgrenzschicht und einem Temperaturprofil dritter Ordnung in der thermischen Grenzschicht. Ein Vergleich wurde angestellt zwischen diesen Ergebnissen und kürzlich veröffentlichten Methoden für konstante Wärmestromdichten durch die Wand.

Аннотация—Представлены локальные коэффициенты переноса тепла от равномерно нагреваемого цилиндра при поперечном течении воды и проведено сравнение с теоретическими данными. Исследовано влияние запирания канала и введена поправка на эффект запирания как для локальных, так и для средних значений теплообмена. Также рассмотрено изменение вязкости в зависимости от температуры поперек пограничного слоя и это влияние учтено отношением вязкости.

Эксперименты проводились в интервале: чисел Рейнольдса от 2000 до 120000, чисел Прандтля от 1 до 7, разности температур среды и поверхности от 20 до 120°F, коэффициента запирания от 0,208 до 0,415. Локальные коэффициенты теплообмена определялись по изменению температуры стенки трубы с помощью термопары, заделанной на внутренней поверхности.

Для анализа теплообмена в ламинарном пограничном слое использовались интегральные методы с профилем скорости Польхаузена в динамическом пограничном слое и профилем температуры, описанным полиномом третьей степени в тепловом пограничном слое. Проведено сравнение результатов настоящей работы с ранее опубликованными методами для случая постоянного теплового потока на стенке.